



Synthesis of (4-Bromo-3-Fluorophenyl)(Pyrimidin-5-yl)Methanol and their Transition Metal Complexes, Spectral, X-ray Powder Diffraction, Cytotoxicity, Molecular Docking, and Biological Evaluation

R. Mohammed Shafeeulla¹, Ganganai Krishna Murthy^{1*}, Halehatti S. Bhojyanaik²,
T. Manjuraj¹, Subba Poojari³

¹Department of Chemistry, Sahyadri Science College (Auto), Shimoga, Karnataka, India, ²Department of Industrial Chemistry, Janna Sahyadri, Kuvempu University, Shankaraghattha, Karnataka, India, ³Syngene International Ltd., Biocon Park, Bengaluru, Karnataka, India.

Received 26th July 2017; Revised 14th August 2017; Accepted 14th August 2017

ABSTRACT

The article deals with a study of a new series of transition metal complexes such as Co^(II), Ni^(II), Cu^(II), and Zn^(II) with pyrimidine-based ligand (4-bromo-3-fluorophenyl)(pyrimidin-5-yl)methanol; the novel ligand has been synthesized through Barbier-type reaction and structurally characterized by ¹H nuclear magnetic resonance, infrared, ultraviolet-visible, and powder X-ray powder diffraction (XRD) spectral techniques. The powder XRD studies reveal that all complexes are in crystalline nature. The cytotoxic activity of the complexes and the uncoordinated ligand against human breast cancer (MCF-7) and chronic myelogenous leukemia cell line (K-562) exhibits good viability in the range of 52.11-66.23% at the concentration >100-110 µg/mL as compared to the inhibition in the untreated cells. The result of antibacterial activity revealed that the complexes of cobalt and copper are active against the studied bacteria and fungi, and the cytotoxicity studies are correlated with the computational docking analysis.

Key words: Barbier reaction, Lithium metal, Sonochemistry.

1. INTRODUCTION

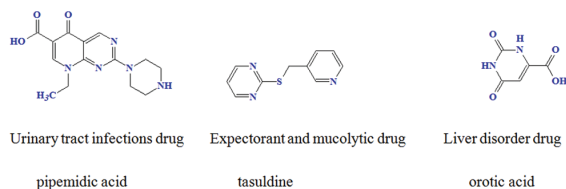
Philippe Barbier reported a coupling reaction between a ketone (6-methyl-5-hepten-2-one) and an alkyl halide (CH₃I) in the presence of a stoichiometric quantity of magnesium metal, thus establishing the basis for the one-step C-C bond forming process is known as the Barbier reaction. The Barbier reaction is an organic reaction between an alkyl halide and the carbonyl group as an electrophilic substrate in the presence of magnesium, aluminum, zinc, indium, tin, or its salts. The reaction product is a primary, secondary, or tertiary alcohol.

Barbier type reaction can be carried out using mixed Mg/Li amides TMPMgCl·LiCl and TMP₂MgCl·LiCl [1-3]. A mixture of zinc [4], aluminum and indium metal [5], bismuth-mediated [6], titanium [7], antimony [8], scandium [9], cobalt [10], cerium [11], silver [12], ionic liquids [13], and tin nano-particles in water [14] developed a new approach for synthesizing homoallyl alcohol.

Pyrimidines are six-membered unsaturated ring compounds composed of carbon and nitrogen, and they are found throughout nature in various form with nitrogen atoms at positions 1 and 3. Pyrimidines are also known as diazine, or 1,3-diazine can be regarded as cyclic amine [15]; pyrimidine, being an integral part of DNA and RNA, has imparted diverse pharmacological properties as an effective bactericide, fungicide [16], anti-inflammatory [17], antioxidant [18], antihypertensive [19], and anticancer [20]. They are back bone in several natural compounds with potent biological activity such as antineoplastic (uramustine, tegafur, and floxuridine), antibacterial (trimethoprim, pyrimidic acid, and metioprim), antifungal (flucytosine), antivirals (broxuridine and idoxuridine) anthelmintic (pyrantel embonate), vasodilators (dipyridamole and trapidil), parkinsonism (piribedil), liposaccharides, and antibiotics [21]. In addition, they play a vital role in the production of several drugs for thyroid, leukemia [22], herbicides [23], pyrimidine derivatives with docking

*Corresponding Author:
E-mail: gkmaiksahyadri@gmail.com

and biological active [24], pyrimidine Schiff base complexes with potent microbial activity [25,26], antifungal [27,28], fluorescence quenching study in proteins, toxicity, and DNA interaction [29], and DNA binding studies [30]. Antioxidant and anticancer [31] many half-sandwich complexes worked as excellent catalyst for hydrogenation and for ring-opening metathesis polymerization [32]. Ni(II) complex acts as catalysts for ethylene polymerization [33], coordination polymers [34], electroactive ligands and complexes [35], and isomerism and geometric [36]. Some drugs are derived from pyramidal moiety.



To the best of our knowledge, no reports have been appeared till date in literature described the interaction of 5-bromopyrimidine and 4-bromo-3-fluorobenzaldehyde (4-bromo-3-fluorophenyl) (pyrimidin-5-yl)methanol (PYM) as ligand and its transition metal complexes. The aim of the present study was to synthesize the PYM through the Barbier reaction, and their transition metal complexes, evaluation of biological activities, and *in silico* molecular docking studies for cytotoxic activities are correlated.

2. EXPERIMENTAL

2.1. Materials and Physical Measurements

All of the chemicals and solvents were purchased from Merck Chemical Company and used as received without further purification, preparative “flash” Silica gel 60, and thin-layer chromatography plates type Silica gel 60 F254 on aluminum sheets were purchased from Merck (Darmstadt, Germany). The human breast cancer (MCF-7) cell line was obtained from the National Center for Cell Science, Pune, India. Infrared (IR) spectra were recorded as KBr pellets in the Bruker Alpha Fourier-transform infrared (FT-IR) spectrometer, ¹H nuclear magnetic resonance (NMR) was recorded on a Bruker DPX 400, and δ values were relative to the deuterated dimethyl sulfoxide (DMSO). Magnetic susceptibilities were measured at room temperature by the Gouy method, and C, H, and N determinations were undertaken using an Elementar Analysis System Gmb H Vario EL II. The molar conductance measurements were measured in a solution of the metal complexes in DMF (10^{-3} M) using Equip-Tronics EQ-660A conductivity meter, and mass spectra are recorded in a Quattro LC, Micro Mass spectrometry. Absorbance is measured using Systronics ultraviolet (UV)-visible spectrometer-119, and grain size of the powdered sample was measured

by X-ray diffractometer (Philips X-pert pro diffractometer, PW 1830) at room temperature with CuK α (1.5418 Å) radiation.

2.2. Synthesis of PYM

The ligand was synthesized according to the literature [37]. 5-bromopyrimidine (6.2 mmol, 1 g) with 4-bromo-3-fluorobenzaldehyde (7.5 mmol, 1.5 g) and the lithium powder (0.013 mol, 0.09 g) were introduced in about 20-30 mL of THF under an atmosphere of dry argon (Scheme 1). The reaction medium was placed in the ultrasound cleaning bath for 40 min. Elimination of the remaining lithium powder was then carried out using 8 mL ethanol. The reaction medium was then diluted with 10 mL of water and evaporated. The aqueous layer was extracted with ethyl acetate (4 \times 10 mL). The organic layer was dried over magnesium sulfate and slowly evaporated. The crude product was purified by column chromatography on silica gel.

It was obtained as lightish-yellow solid in 59% yield; mp. 138-142°C; IR (KBr, cm^{-1}): 3395 (-OH), 1594 (C=N), 1489 (C=C), ¹H NMR: (400 Mz, DMSO- d_6 , ppm): δ 3.18 (s, 1H, CH), 4.05 (broad, 1H, -OH), 7.21-8.70 (m, 6H, Ar-H) (Figure 1), MS (m/z): 283.0.

2.3. Synthesis of Metal Complexes [1-4]

A hot methanolic solution of metal chlorides (0.331 g, 0.014 mol) in 10 mL was added dropwise to the methanolic solution (10 mL) of ligand (0.8 g, 0.002 mol) with continuous stirring (Scheme 2). The resulting solution was refluxed for 4-6 h, and the solution was reduced to half of its initial volume. It was then allowed to stand overnight in a refrigerator. A colored complex was precipitated, which was separated by filtration under vacuum. It was washed thoroughly with distilled water then with cold methanol and dried *in vacuo* over fused CaCl₂ and was recrystallized from methanol [38].

[CuL₂Cl₂] (1): Green; yield 68%; mp, >212-214°C; mw, 698.6 g/mol; found for C₂₂H₁₄Br₂Cl₂CuF₂N₄O₂: C: 39.17; H: 2.68; N: 8.09; M: 9.15, calculated for C: 39.07; H: 2.65; N: 8.11, and M: 9.18. UV-visible (DMF): λ_{max} (log ϵ) = 19,920. FT-IR (KBr/(cm^{-1}): ν (C=N)1572, ν (C=C) 1488, ν (M-O) 509, ν (M-N) 477. $\Lambda_{\text{M}} = 60.31 \Omega^{-1} \cdot \text{cm}^2 \cdot \text{mol}^{-1}$.

[CoL₂Cl₂] (2): Lightish brown; yield 63 %; mp, >210-213°C; mw, 694.0 g/mol; found for C₂₂H₁₄Br₂Cl₂CoF₂N₄O₂: C: 39.24; H: 2.10; N: 8.11; M: 8.09, calculated for C: 39.17; H: 2.15; N: 8.14, M: 8.11. UV-visible (DMF): λ_{max} (log ϵ) = 16,339, 14,534. FT-IR (KBr/(cm^{-1}): ν (C=N)1573, ν (C=C) 1481, ν (M-O) 509, ν (M-N) 477. $\Lambda_{\text{M}} = 50.31 \Omega^{-1} \cdot \text{cm}^2 \cdot \text{mol}^{-1}$.

[NiL₂Cl₂] (3): Pale green; yield 60%; mp, >208-210°C; mw, 693.8 g/mol; found for C₂₂H₁₄Br₂Cl₂NiF₂N₄O₂:

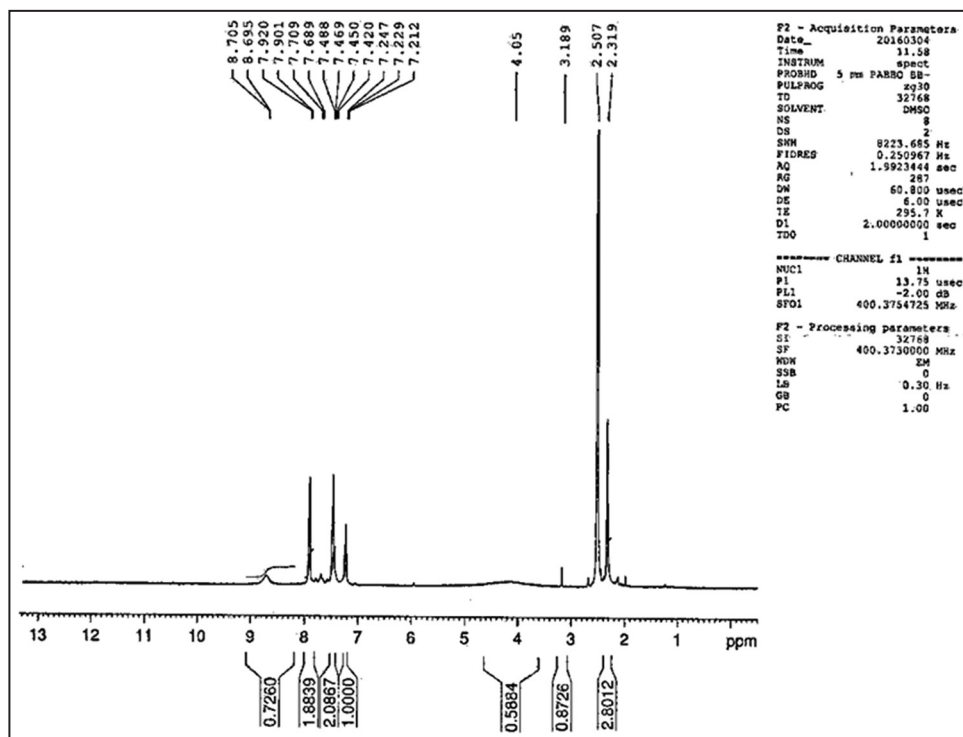
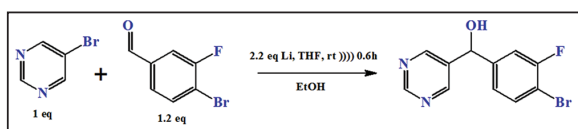
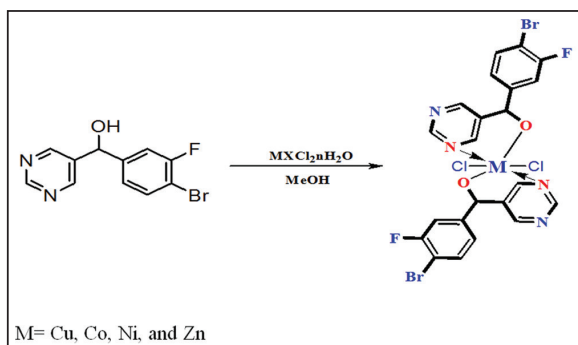


Figure 1: ¹H nuclear magnetic resonance spectrum of (4-bromo-3-fluorophenyl)(pyrimidin-5-yl)methanol.



Scheme 1: Synthesis of (4-bromo-3-fluorophenyl)(pyrimidin-5-yl)methanol.



Scheme 2: Synthesis of metal complexes.

C: 39.11; H: 2.48; N: 8.09; M: 8.48, calculated for C: 39.06; H: 2.51; N: 8.07; M: 8.52. UV-visible (DMF): λ_{\max} ($\log \epsilon$) = 25,000, 2,00,015, 3840. FT-IR (KBr/ cm^{-1}): $\nu(\text{C}=\text{N})$ 1531, $\nu(\text{C}=\text{C})$ 1480, $\nu(\text{M}-\text{O})$ 509, $\nu(\text{M}-\text{N})$ 477. $\text{AM} = 52.31 \Omega^{-1} \cdot \text{cm}^2 \cdot \text{mol}^{-1}$.

[ZnL₂Cl₂] (4): Cremish White; yield 62%; mp, >214-216°C; mw, 700.05 g/mol; found for C₂₂H₁₄Br₂Cl₂F₂N₄O₂Zn: C: 39.27; H: 2.58; N: 8.10; M: 9.35, calculated for C: 39.19; H: 2.55; N: 8.09; M: 9.28. FT-IR(KBr/ cm^{-1}): $\nu(\text{C}=\text{N})$ 1577, $\nu(\text{C}=\text{C})$

1489, $\nu(\text{M}-\text{O})$ 509, $\nu(\text{M}-\text{N})$ 477. $\text{AM} = 55.38 \Omega^{-1} \cdot \text{cm}^2 \cdot \text{mol}^{-1}$.

2.4. Molecular Docking Studies

Molecular docking of the synthesized compounds has been evaluated as per the previous work [39-41]. For cytotoxic molecular docking study (PDB code: 2A91), as EGFR kinase domain was used throughout the work, followed by actinoin as standards for docking studies, the docking results of the cytotoxic guided for wet analysis.

2.5. Antimicrobial Activity

All the synthesized complexes and ligand have been examined toward three bacterial and fungal strains using agar well-diffusion method [42]. All bacterial traces were maintained on nutrient agar medium at $\pm 37^\circ\text{C}$, and fungal strains were maintained on potato dextrose agar at $\pm 25^\circ\text{C}$. The test compounds had been dissolved in DMSO. Sample-loaded plates were inoculated with the microorganism incubated at 37°C for 24 h, and culture was incubated at 25°C for 60 h. DMSO as control and chloramphenicol and fluconazole is used as standards for bactericidal and fungicide. The compounds were also tested for minimal inhibitory concentration (MIC) values [43].

2.6. Antioxidant Activity

The free radical scavenging activity of the ligand PYM and complexes was measured *in vitro* by 2, 2'-diphenyl-1-picrylhydrazyl (DPPH) assay. The stock solution was prepared by dissolving 24 mg DPPH

with 100 ml methanol and stored at 20°C until required. The working solution was obtained by diluting DPPH solution with methanol to attain an absorbance of about 0.98 ± 0.02 at 517 nm, and using the spectrophotometer, all the tested samples in various concentrations (50, 75, and 100 $\mu\text{g/mL}$) were prepared in methanol, and the homogeneous solutions were achieved by stirring. Aliquot of test sample (1 mL) was added to 4 mL of 0.004% (w/v) methanol solution of DPPH, and then, reaction mixture was vortexed for 1 min and kept at room temperature for 30 min in the dark to complete the reaction. The absorbance was read against blank at 517 nm. The synthetic antioxidant BHT was used as positive control. The ability of the tested samples at tested concentration to scavenge DPPH radicals was calculated using the following equation [44].

$$\text{Scavenging ratio (\%)} = [(A_i - A_0) / (A_c - A_0)] \times 100\%$$

Where A_i is the absorbance in the presence of the test compound; A_0 is absorbance of the blank in the absence of the test compound; A_c is the absorbance in the absence of the test compound.

2.7. In vitro Anticancer Activity-cell Culture

The human cancer cells (K-562 ATCC® CCL-243™) and (MCF7-ATCC® HTB 22™) were maintained in modified eagles medium supplemented with 10% FCS, 2% essential amino acids, 1% each of glutamine, nonessential amino acids, vitamins, and 100 U/mL penicillin–streptomycin. Cells were subcultured at 80–90% confluence and incubated at 37°C in a humidified incubator supplied with 5% CO_2 . The stock cells were maintained in 75 cm^2 tissue culture flask. The cytotoxicity effect of test samples was performed by 5-diphenyl-2H-

tetrazolium bromide (MTT) assay. Briefly, cultured cells (1×10^6 cells/mL) were placed in 96 flat-bottom well plates; then, cells were exposed to different concentration of prepared samples (1–100 $\mu\text{g/mL}$) and incubated at 37°C for about 24 h in 5% CO_2 atmosphere. After 24 h incubation, MTT (10 μL) was added to the incubated cancer cells and further incubated at 37°C for about 4 h in the same environment. Thereafter, dissolved 200 μL of formazan crystals in of DMSO and monitored the absorbance at 578 nm with reference filter as 630 nm. The cytotoxicity effect was calculated as follows:

$$\text{Cytotoxicity (\%)} = 1 - \left[\frac{\text{Mean absorbance of positive}}{\text{Mean absorbance of negative}} \right] \times 100$$

$$\text{Cell viability (\%)} = 100 - \text{Cytotoxicity (\%)}$$

3. RESULTS AND DISCUSSION

3.1. Mass Spectrum

The mass spectrum of the ligand (Figure 2) obtained using Quattro LC; micro mass spectrophotometer showed the molecular ion peak at m/z 283.0 which matches with formula weight within the precision limit of ± 0.02 . Metastable ion(s) which is not observed represents the proposed fragmentation pattern of the ligand.

3.2. IR Spectroscopy

A comparative IR spectral study of the ligand (Figure 3) and its metal complexes has been recorded as KBr pellets (Figures 4 and 5). Some significant IR bands for the uncoordinated ligand and their metal complexes have been said above. The free ligand showed a strong band at 3395 cm^{-1} and a weak band at 3062 cm^{-1} which are attributed to $\nu(\text{-OH})$ and $\nu(\text{C-H})$, respectively, of

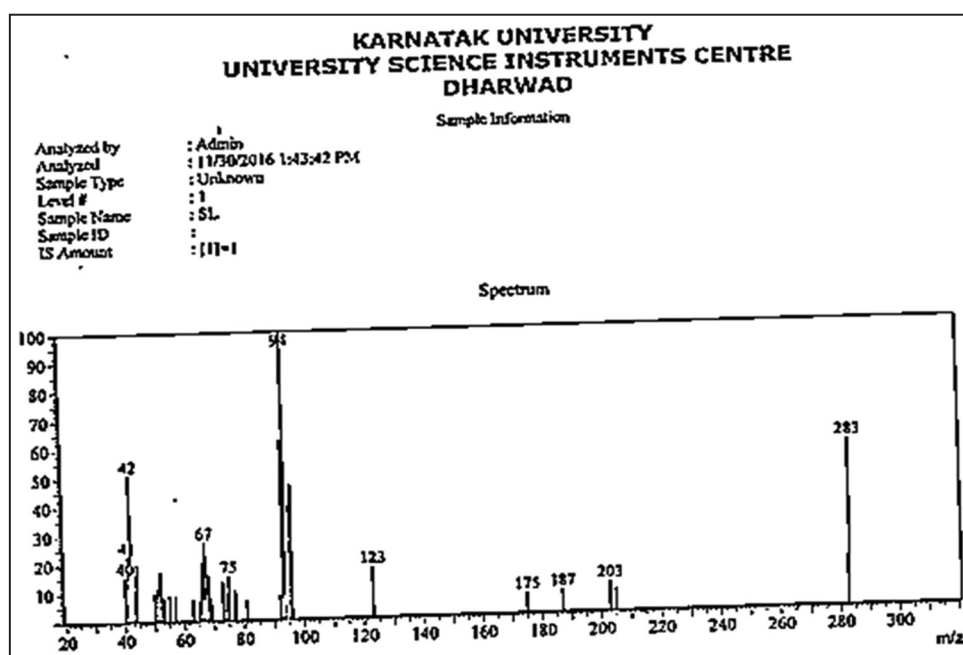


Figure 2: Mass spectrum of ligand (4-bromo-3-fluorophenyl)(pyrimidin-5-yl)methanol.

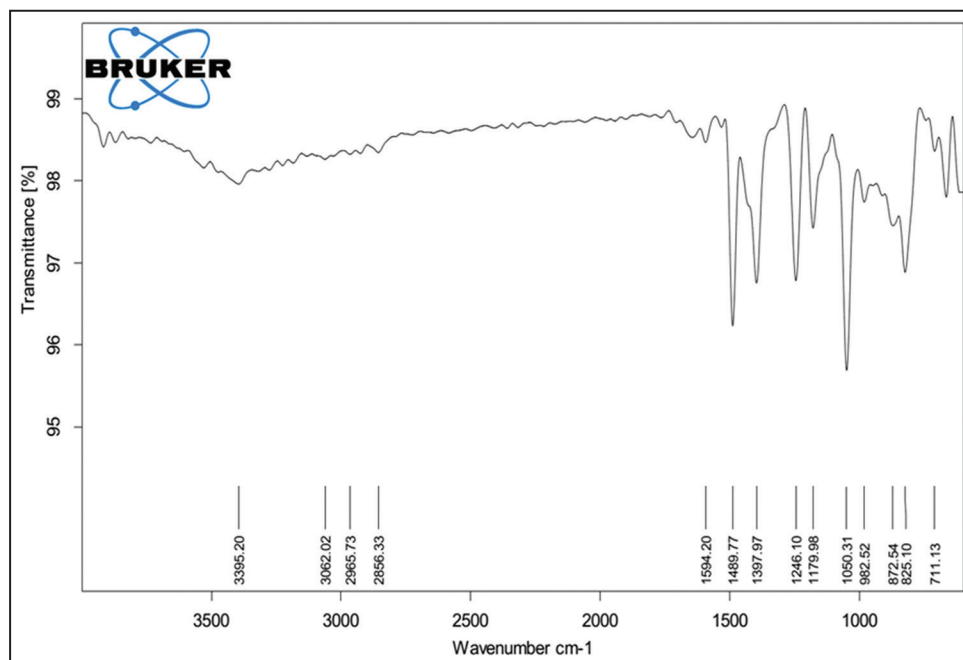


Figure 3: Infrared spectrum of ligand ((4-bromo-3-fluorophenyl)(pyrimidin-5-yl)methanol).

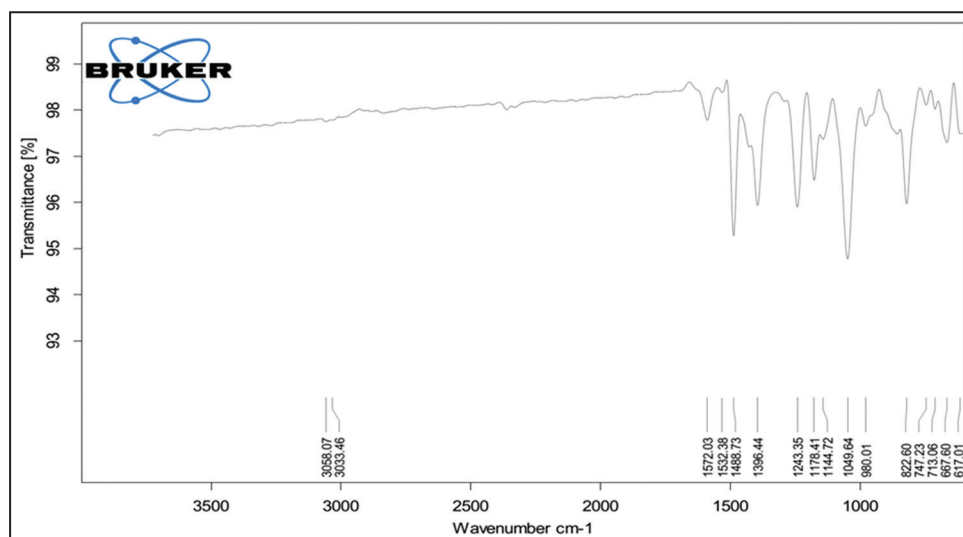


Figure 4: Infrared spectrum of complex 1.

the aromatic group [45]. The IR spectrum of the ligand displayed a band at 1594 cm^{-1} due to the $\nu(\text{C}=\text{N})$ of pyrimidine ring [46]. In the spectrum of the ligand, the hypsochromic shift was observed for the $\nu(\text{C}=\text{N})$ band at 1.594 cm^{-1} assigned in the spectrum of the ligand. In the spectra of the complexes, the band due to $\nu(\text{C}=\text{N})$ showed a reduction in intensities between 1.594 and 1.531 cm^{-1} region observed due to the coordination to central metal ions [47] after the deprotonation of the hydroxyl group in the metal complexes [48]. In addition, the band due to cyclic($\text{C}=\text{C}$) of ring was little bit shifted in all complexes. This shift indicates the involvement of the nitrogen in the coordination. This was further supported by the existence of new metal-ligand band in the complex spectrum ranging

from $509\text{-}511\text{ cm}^{-1}$ for M-O band and $474\text{-}477\text{ cm}^{-1}$ for M-N.

3.3. Electronic Spectra and Magnetic Moment Measurements

The molar conductance value indicates that all metal complexes behave as uni-bivalent nature. The UV-visible spectrum of the ligand and their metal complexes are recorded in DMF, and the values are reported in Table 1. The free ligand showed two recognizable absorption bands at $36,363$ and $32,362\text{ cm}^{-1}$ which would be due to the $\pi\text{-}\pi^*$ and $n\text{-}\pi^*$ transitions, respectively. The spectrum of the Cu(II) complex [1] showed an absorption band at $19,920\text{ cm}^{-1}$ attributed to the transition ${}^2\text{E}_g \rightarrow {}^2\text{T}_{2g}$

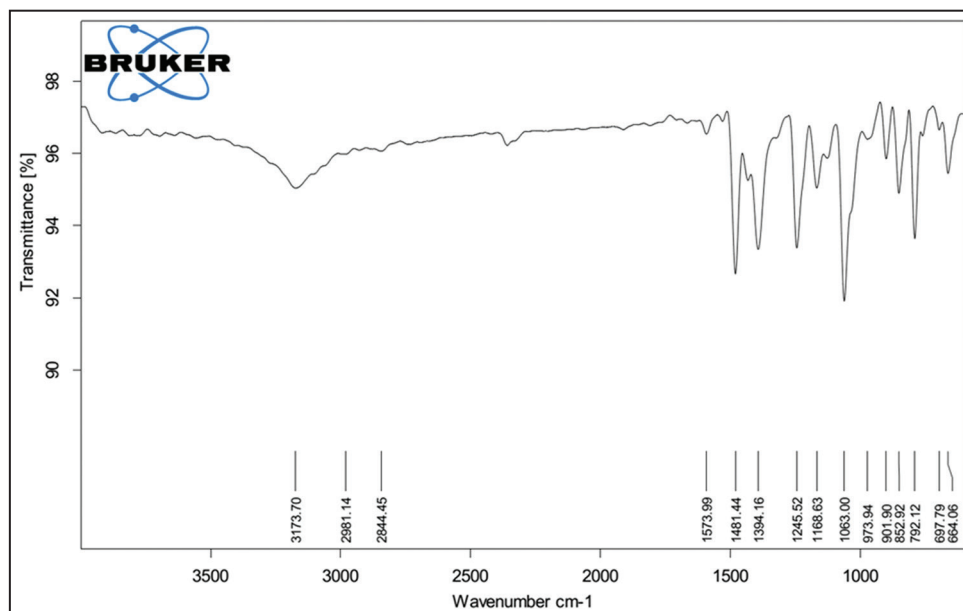


Figure 5: Infrared spectrum of complex 2.

and the magnetic moment values 1.77 B.M [49,50] which is consistent with proposed distorted octahedral geometry for Cu(II) complex. The Co(II) complex [2] showed absorption band at $14,534\text{ cm}^{-1}$ and $16,339\text{ cm}^{-1}$ due to the transitions ${}^4T_{1g}(F) \rightarrow {}^4A_{2g}(F)$ and ${}^4T_{1g}(F) \rightarrow {}^4A_{2g}(P)(\nu_2)$, respectively, and the Co(II) complex also showed a magnetic moment at 4.57 B.M. These results suggested the presence of octahedral geometry for Co(II) complex [51,52]. The Ni(II) complex [3] showed three bands at $25,000\text{ cm}^{-1}$, $20,000\text{ cm}^{-1}$, and $15,384\text{ cm}^{-1}$ which are assignable to ${}^3A_{2g}(F) \rightarrow {}^3T_{2g}(F)(\nu_1)$, ${}^3A_{2g}(F) \rightarrow {}^3T_{1g}(F)(\nu_2)$, and ${}^3A_{2g}(F) \rightarrow {}^3T_{1g}(P)(\nu_3)$ transitions, respectively. The spectral data indicate that the Ni(II) ion is present in octahedral environment. The magnetic moment of Ni(II) complex is 2.74 B.M [53,54].

3.4. Powder X-ray Diffraction Study of Complexes

Powder X-ray diffract graph of the complexes was recorded over the $2\theta = 0-80^\circ$ range. The major peaks of relative intensity $>10\%$ were indexed using a computer program. The diffraction data such as angle (2θ), interplanar spacing (d), and relative intensity (%) have been summarized in Table 2, and from the data, all compounds show sharp crystalline peaks indicating their crystalline nature (Figure 6). The X-ray powder diffraction (XRD) patterns of all complexes are very similar and suggest that the complexes have identical structure. The average crystallite sizes of the complexes were calculated using the Sherrer's formula [51]. The complexes 1, 2, 3, and 4 have a crystallite size of 17.99, 27.33, 31.33, and 26.03 nm, respectively, suggesting that the complexes are in a monoclinic crystalline system (Table 2), and the X-ray diffraction data of complex 1 are shown in Table 3.

Table 1: Electronic spectral data (cm^{-1}) and magnetic values of PYM and its metal complexes.

| Entry | Transitions (cm^{-1}) | Transitions | μ_{eff} (BM) |
|-------|----------------------------------|--|-------------------------|
| PYM | 36,363 | $\pi-\pi^*$ | - |
| | 32,362 | $n-\pi^*$ | |
| 1 | 19,920 | ${}^2E_g \rightarrow {}^2T_{2g}$ | 1.77 |
| 2 | 16,339 | ${}^4T_{1g}(F) \rightarrow {}^4A_{2g}(P)(\nu_2)$ | 4.57 |
| | 14,534 | ${}^4T_{1g}(F) \rightarrow {}^4A_{2g}(F)$ | |
| 3 | 25,435 | ${}^3A_{2g}(F) \rightarrow {}^3T_{2g}(F)(\nu_1)$ | 2.74 |
| | 20,000 | ${}^3A_{2g}(F) \rightarrow {}^3T_{1g}(F)(\nu_2)$ | |
| | 15,384 | ${}^3A_{2g}(F) \rightarrow {}^3T_{1g}(P)(\nu_3)$ | |
| 4 | Dia | | Dia |

PYM: (4-Bromo-3-Fluorophenyl)(Pyrimidin-5-yl) Methanol

Table 2: PXRD spectral data of 1-4.

| Complexes | 2θ | d | Relative intensity | Full width at half maximum |
|-----------|-----------|------|--------------------|----------------------------|
| 1 | 26.69 | 3.33 | 100 | 0.4742 |
| 2 | 26.52 | 3.35 | 100 | 0.3119 |
| 3 | 26.66 | 3.34 | 100 | 0.2722 |
| 4 | 25.32 | 3.51 | 100 | 0.3268 |

3.5. Antimicrobial Activity

All the complexes including ligand showed inhibition property, among them, the complexes 1

and 2 showed excellent antibacterial activity when compared to the standard (Table 4). The result of MIC values $<25 \mu\text{g/mL}$ is presented in Table 5. The antifungal activity results indicate that the PYM and complexes 3, 4 exhibited the least activity and the other two complexes 1 and 2 showed promising activity.

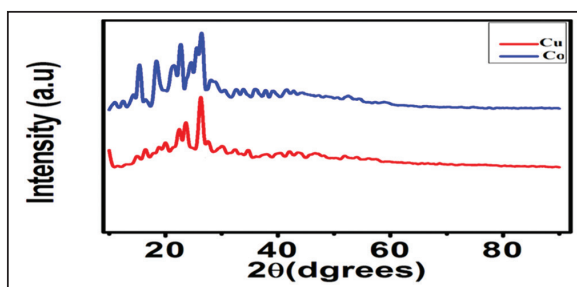


Figure 6: Powder X-ray powder diffraction spectrum of complexes 1 and 2.

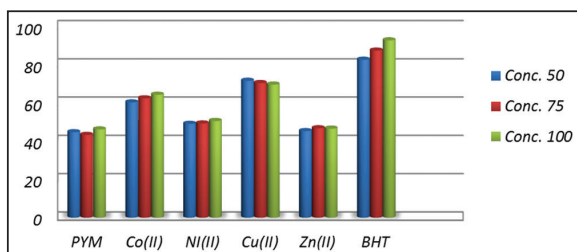


Figure 7: Antioxidant activity DPPH method.

3.6. Antioxidant Activity

The antioxidant activities of the metal complexes and ascorbic acid (standard) as found by scavenging DPPH radical are shown in Figure 7. When the concentration of compounds was increased from $50 \mu\text{g/ml}$ to $100 \mu\text{g/ml}$, DPPH radical scavenging activities were increased. The $\text{Co}(\text{II})$ and $\text{Cu}(\text{II})$ complexes showed excellent DPPH radical scavenging activity, whereas the $\text{Ni}(\text{II})$, $\text{Zn}(\text{II})$, and ligand PYM showed moderate inhibition. The radical scavenging activity of the compound depends on the structural factors such as hydroxyl and other structural features present in the coordination of ligand to the metal ions. The order of antioxidant activity of the complexes is $\text{ascorbic acid} > \text{Cu}(\text{II}) > \text{Co}(\text{II}) > \text{Ni}(\text{II}) > \text{Zn}(\text{II}) > \text{PYM}$.

3.7. Molecular Docking Study

The EGFR tyrosine kinase was reported several times as target for the inhibition of cancer cells. Therefore, all the four complexes used to study the effect docking inside the active site of EGFR kinase domain with a binding energy values in the range of -272 – $-314 \text{ kcal mol}^{-1}$ as tabulated in Table 6. The molecular docking results revealed that complex 1 has the best binding energy values $-314 \text{ kcal mol}^{-1}$ for the EGFR kinase domain inhibited complex formation by forming a four hydrogen bonds with GLY7 with bond distances 0.66 \AA , 2.58 \AA , 2.66 \AA , and 2.75 \AA ; three hydrogen bonds with THR8 with bond distances 1.79 \AA , 2.95 \AA , and 3.11 \AA ; two more hydrogen bonds with three

Table 3: X-ray diffraction data of 1.

| Peak No. | 2θ | θ | $\text{Sin}\theta$ | h k l | d | | Intensity | a in \AA |
|----------|-----------|----------|--------------------|-------|---------|--------|-----------|-------------------|
| | | | | | Cal | Obs | | |
| 1 | 12.02 | 6.01 | 0.1047 | 462 | 7.35443 | 7.3544 | 160.92 | 3.62 |
| 2 | 14.30 | 7.15 | 0.1244 | 469 | 6.18663 | 6.1865 | 100.83 | 3.62 |
| 3 | 14.77 | 7.385 | 0.1285 | 711 | 5.99109 | 5.9911 | 164.94 | 3.62 |
| 4 | 15.26 | 7.63 | 0.1327 | 702 | 5.79892 | 5.7981 | 185.13 | 3.62 |
| 5 | 16.07 | 8.035 | 0.1397 | 721 | 5.50830 | 5.5082 | 434.99 | 3.62 |
| 6 | 16.66 | 8.33 | 0.1448 | 827 | 5.31470 | 5.3146 | 200.72 | 3.62 |
| 7 | 18.11 | 9.055 | 0.1573 | 450 | 4.89402 | 4.8939 | 48.89 | 3.62 |
| 8 | 19.20 | 9.6 | 0.1667 | 120 | 4.61859 | 4.6185 | 407.78 | 3.62 |
| 9 | 20.12 | 10.06 | 0.1746 | 837 | 4.40956 | 4.4095 | 198.65 | 3.62 |
| 10 | 26.69 | 13.345 | 0.2308 | 237 | 3.33660 | 3.3365 | 989 | 3.62 |
| 11 | 30.19 | 15.095 | 0.2604 | 553 | 2.95710 | 2.9570 | 136.52 | 3.62 |
| 12 | 31.92 | 15.96 | 0.2749 | 454 | 2.80065 | 2.8006 | 75.58 | 3.62 |
| 13 | 33.16 | 16.58 | 0.2853 | 362 | 2.69969 | 2.6996 | 40.09 | 3.62 |
| 14 | 35.89 | 17.945 | 0.3081 | 413 | 2.50001 | 2.5000 | 62.37 | 3.62 |
| 15 | 37.59 | 18.795 | 0.3221 | 410 | 2.39050 | 2.3904 | 96.78 | 3.62 |
| 16 | 39.35 | 19.675 | 0.3366 | 480 | 2.28740 | 2.2873 | 82.15 | 3.62 |
| 17 | 42.74 | 21.37 | 0.3643 | 361 | 2.11390 | 2.1138 | 60.44 | 3.62 |
| 18 | 48.15 | 24.075 | 0.4079 | | 1.88799 | 1.8879 | 91.68 | 3.62 |

Table 4: Antimicrobial data of PYM and their complexes.

| Entry | Antibacterial zone of inhibition in mm (mean±SD) | | | Antifungal zone of inhibition in mm (mean±SD) | | |
|-----------------|--|--------------------------|-------------------------|---|-------------------------|--------------------------|
| | <i>Staphylococcus aureus</i> | <i>Bacillus subtilis</i> | <i>Escherichia coli</i> | <i>Staphylococcus coccus</i> | <i>Candida albicans</i> | <i>Aspergillus niger</i> |
| PYM | 03±0.3 | 05±0.2 | 05±0.7 | 05±0.4 | 04±0.1 | - |
| 1 | 13±0.1 | 15±0.1 | 12±0.3 | 08±0.4 | 09±0.1 | 08±0.3 |
| 2 | 14±0.3 | 12±0.4 | 10±0.2 | 07±0.2 | 08±0.3 | 07±0.3 |
| 3 | 06±0.2 | - | 0.7±0.3 | 05±0.6 | - | 04±0.3 |
| 4 | 05±0.1 | 10±0.1 | 06±0.1 | 05±0.1 | 03±0.1 | 05±0.1 |
| Chloramphenicol | 15±0.2 | 16±0.3 | 13±0.3 | 12±0.2 | 11±0.4 | 13±0.3 |
| Fluconazole | - | - | - | 16±0.2 | 12±0.1 | 11±0.3 |
| DMSO | 0 | 0 | 0 | 0 | 0 | 0 |

SD: Standard deviation, PYM: (4-Bromo-3-Fluorophenyl)(Pyrimidin-5-yl) Methanol

Table 5: Antimicrobial activity.

| Entry | MIC of the compounds in 25 µg/mL | | | | | |
|-------|----------------------------------|--------------------------|-------------------------|------------------------------|-------------------------|--------------------------|
| | <i>Staphylococcus aureus</i> | <i>Bacillus subtilis</i> | <i>Escherichia coli</i> | <i>Staphylococcus coccus</i> | <i>Candida albicans</i> | <i>Aspergillus niger</i> |
| PYM | 10 | - | 12 | 09 | 08 | - |
| 1 | 19 | 20 | 22 | 17 | 13 | 22 |
| 2 | 17 | 21 | 17 | 19 | 12 | 15 |
| 3 | 13 | 13 | 14 | 11 | 09 | 10 |
| 4 | 11 | 14 | 13 | 08 | 06 | 09 |

PYM: (4-Bromo-3-Fluorophenyl)(Pyrimidin-5-yl) Methanol

Table 6: Cytotoxic docking scores.

| Entry | Receptor PDB code | ΔG (Kcal/mol) With MurB |
|----------------|-------------------|-------------------------|
| PYM | 2A91 | -192.37 |
| 1 | 2A91 | -314.98 |
| 2 | 2A91 | -292.85 |
| 3 | 2A91 | -284.97 |
| 4 | 2A91 | -272.12 |
| Actinoin (STD) | 2A91 | -235.99 |

PYM: (4-Bromo-3-Fluorophenyl)(Pyrimidin-5-yl) Methanol

different amino acids are THR6, ASP9, and MET10 with bonds distances 2.78 Å, 2.80 Å; 2.48 Å, 3.01 Å; and 1.62 Å, 1.76 Å, respectively, and finally, a single hydrogen bonds with three different amino acids are ASN38, LYS11, and GLY37 with bond distances 2.19 Å, 2.91 Å, and 2.96 Å, respectively. The other interacting amino acids were ASN467, SER442, GLY418, ASN467, ASN38, THR8 and GLY418, ASN417, GLU40, LEU28, LEU415, and TYR29 as shown in Figure 8. The complex 2 (-292 kcal mol⁻¹) formed three hydrogen bonds with GLY7 with bonds distances are 2.02 Å, 2.60 Å, and 3.05 Å and two

more hydrogen bonding with two different amino acids are THR8 and ALA419 with bonds distances are 1.80 Å, 2.04 Å and 2.28 Å, 3.15 Å, respectively. The other interacting amino acids were ARG13, GLY37, GLN36, GLY37, GLN36, THR8, HIS469, ALA419, LEU415, and LEU28 as shown in Figure 9. Even though the complexes 3 (-284 kcal mol⁻¹) and 4 (-272 kcal mol⁻¹) are having good docking energy values than the standard actinoin (-235.99 kcal mol⁻¹), these complexes were not forming having hydrogen bonding interactions with EGFR tyrosine kinase receptor than complexes 1 and 2. The complexes 3 and 4 interact with active sites of EGFR tyrosine kinase with amino acid residues are ARG13, GLY37, GLN36, GLY37, GLN36, THR8, HIS469, ALA419, LEU415, and LEU28.

The binding value of complexes 1 and 2 showed the better cytotoxicity property than the rest of complexes. The obtained results provide a sufficient explanation and good compromise between docking scores and *in vitro* results of antibacterial and cytotoxicity activity.

3.8. Cytotoxicity

The results of cytotoxic activity are tabulated in Table 7; the reliable criteria for judging the efficacy of any anticancer drug are the prolongation of lifespan,

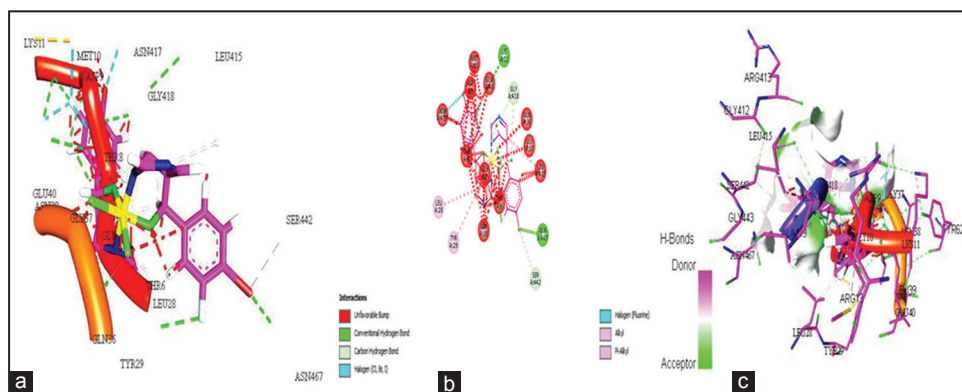


Figure 8: Interaction of 1 with amino acids of 2A91 (a), (b) 3D and 2D interactions 1 (ball and stick model oxygen-red, nitrogen-blue) protein receptor (stick model) structure of the complex (c) structure with hydrogen bonding.

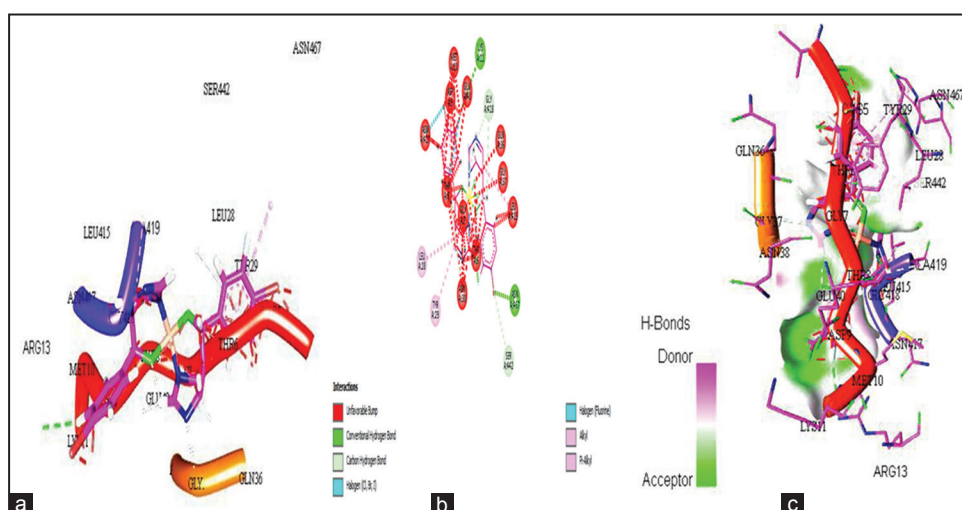


Figure 9: Interaction of 1 with amino acids of 2A91 (a), (b) 3D and 2D Interactions 1 (ball and stick model oxygen-red, nitrogen-blue) protein receptor (stick model) structure of the complex (c) structure with hydrogen bonding.

Table 7: Cytotoxicity activity of ligand and complexes.

| Tested samples | Inhibitory effect on cell lines (IC ₅₀) | |
|----------------|---|--------------------|
| | MCF-7 (%) | K-562 (%) |
| PYM | >120 µg/mL (53.38) | >120 µg/mL (52.11) |
| 1 | 110 µg/mL (65.16) | 100 µg/mL (63.42) |
| 2 | 120 µg/mL (64.79) | 110 µg/mL (66.23) |
| 3 | 100 µg/mL (55.19) | 90 µg/mL (54.36) |
| 4 | 80 µg/mL (52.16) | 90 µg/mL (53.12) |

PYM: (4-Bromo-3-Fluorophenyl)(Pyrimidin-5-yl) Methanol

improving the clinical, hematological, biochemical profile, and reduction in viable tumor cell count in the host. In order to evaluate the biological effects of the ligand, and its 1, 2, 3 and 4 on cancer cells to treat human breast cancer (MCF7) and K-562 cell lines at the concentrations of 80, 90, 100, 110, 120, >130 and

>200 µg/mL for 48 h. The untreated cells were used as a control. The cell growth inhibition was analyzed by the MTT assay, and the results showed that the complexes and the ligand exhibited an inhibitory effect on the proliferation of MCF7 and K-562 cell lines in a dose-dependent manner. Among them, complexes 1 and 2 showed the most potent inhibitory effect on the growth of both the MCF-7 and K-562 cells lines compared to the uncoordinated ligand.

4. CONCLUSION

In this study, a novel ligand (4-bromo-3-fluorophenyl) (pyrimidin-5-yl) methanol (PYM) has been synthesized through Barbier type reaction, and a series of Cu^(II), Co^(II), Ni^(II), and Zn^(II) ion complexes has been prepared and structurally characterized. The deprotonated pyrimidine moiety acted as a bidentate ON-donor ligand, and the complexes Cu^(II) and Co^(II) showed significantly enhanced antibacterial and antifungal activity against microbial and antifungal strains in comparison to free ligand and the rest

of complex. The uncoordinated ligand and metal complexes are screened for antioxidant activity, among them, Cu^(II), Co^(II), and Ni^(II) complexes showed fairly good activity in DPPH scavenging. The results of computational docking studies promote to evaluate *in vitro* cytotoxic activity. The Cu^(II) and Co^(II) complexes exhibited more *in vitro* cytotoxic activity with highest efficacy and exhibited >66% inhibition, and finally, all complexes are crystalline nature. Nevertheless, this research work could be a good start point to further studies.

5. REFERENCES

1. M. Mosrin, N. Boudet, P. Knochel, (2008) Regio- and chemoselective magnesiation of protected uracils and thioracils using TMPMgCl·LiCl and TMP₂Mg·2LiCl, *Organic and Biomolecular Chemistry*, **6**: 3237-3239.
2. A. Kolarovic, (2013) *Topics in Heterocyclic Chemistry, Metalation of Azines and Diazines*, Vol. 31. Berlin, Heidelberg: Springer, p1-20.
3. M. Mosrin, P. Knochel, (2008) Regio- and chemoselective multiple functionalization of pyrimidine derivatives by selective magnesiations using TMPMgCl·LiCl, *Organic Letters*, **10**: 2497-2500.
4. C. Reddy, S. A. Babu, R. Padmavathi, (2016) The barbier-type allylation/lactamization cascade route to isoindolinones and the heck-type annulation route to isoindolo[2,1-*a*]quinolines, *Chemistry Select*, **1(11)**: 2952-2959.
5. T. Moragas, A. Correa, R. Martin, (2014) Metal-catalyzed reductive coupling reactions of organic halides with carbonyl-type compounds, *Chemistry-A European Journal*, **20(27)**: 8242-8258.
6. Y. Wen, G. Chen, S. Huang, Y. Tang, J. Yang, Y. Zhang, (2016) The Barbier-Grignard-type arylation of ketones and unexpected cross-coupling of phenolic ketones using unactivated aryl bromides, *Advanced Synthesis and Catalysis*, **358(6)**: 947-957.
7. N. M. Padiál, C. Hernández-Cervantes, J. Muñoz-Bascón, E. Roldan-Molina, M. García-Martínez, A. B. Ruiz-Muelle, A. Rosales, M. Álvarez-Corral, M. Muñoz-Dorado, I. Rodríguez-García, J. E. Oltra, (2017) Ti-catalyzed synthesis of exocyclic allenes on oxygenated heterocycles, *European Journal of Organic Chemistry*, **2017(3)**: 639-645.
8. X. Y. Shi, W. J. Han, C. J. Li, (2016) Transition-metal-catalyzed direct addition of aryl C-H bonds to unsaturated electrophiles, *The Chemical Record*, **16(3)**: 1178-1190.
9. T. Aklyama, J. Iwai, M. Sugano, (1999) Scandium trifluoromethanesulfonate-catalyzed chemoselective allylation reactions of carbonyl compounds with tetraallylgermane in aqueous media, *Tetrahedron*, **55**: 7499-7508.
10. M. K. Chaudhuri, S. K. Dehury, S. Hussain, (2005) Boric acid: A novel and safe catalyst for aza-michael reactions in water, *Tetrahedron Letters*, **46**: 6247-6251.
11. S. Yadav, B. V. S. Reddy, G. Kondaji, J. S. S. Reddy, (2005) Chemo selective allylation of aldehydes using CeCl₃·7H₂O-a facile synthesis of homoallylic alcohols, *Tetrahedron*, **61**: 879-882.
12. N. T. Barczak, E. R. Jarvo, (2008) Silver-Catalyzed, manganese-mediated allylation and benzylation reactions of aldehydes and ketones, *European Journal of Organic Chemistry*, **33**: 5507-5510.
13. L. Tang, L. Ding, W. X. Chang, J. Li, (2006) SnCl₂-mediated carbonyl allylation of aldehydes and ketones in ionic liquid, *Tetrahedron Letters*, **47**: 303-306.
14. Z. Zha, S. Qiao, J. Jiang, Y. Wang, Q. Miao, Z. Wang, (2005) Barbier-type reaction mediated with tin nano-particles in water, *Tetrahedron*, **61**: 2521-2527.
15. I. L. Finar, (1975) *Organic Chemistry, Stereochemistry and the chemistry of Natural Products*, London: Longman, p2.
16. A. A. Fayed, G. A. E. E-Amr, M. A. AL-Omar, E. E. Mostafa, (2014) Synthesis and antimicrobial activity of some new substituted pyrido [3',2':4,5] thieno [3,2-*d*]pyrimidinone derivatives, *Russian Journal of Bioorganic Chemistry*, **40**: 308-313.
17. H. H. Kadry, (2014) Synthesis, biological evaluation of certain pyrazolo [3,4-*d*] pyrimidines as novel anti-inflammatory and analgesic agents, *Medicinal Chemistry Research*, **23**: 5269-5281.
18. Y. Kotaiah, N. Harikrishana, K. Nagaraju, V. Rao, (2012) Synthesis and antioxidant activity of 1,3,4-oxadiazole tagged thieno[2,3-*d*] pyrimidine derivatives, *European Journal of Medicinal Chemistry*, **58**: 340-345.
19. R. N. Sharma, R. Patel, (2014) Synthesis and pharmacological evaluation of 2-oxo-1,2,3,4-tetrahydropyrimidine-5-carboxylate derivatives as alpha receptor blockers, *International Journal of Pharmtech Research*, **6**: 129-136.
20. Z. Liu, S. Wu, Y. Wang, R. Li, J. Wang, L. Wang, Y. Zhao, P. Gong, (2014) Design, synthesis and biological evaluation of novel thieno[3,2-*d*] pyrimidine derivatives possessing diaryl semicarbazone scaffolds as potent antitumor agents, *European Journal of Medicinal Chemistry*, **87**: 782-793.
21. J. Rani, S. Kumar, M. Saini, J. Mundlia, P. K. Verma, (2016) Biological potential of pyrimidine derivatives in a new era, *Research on Chemical Intermediates*, **42**: 6777-6804.
22. A. Bishnoi, S. Singh, A. K. Tiwari, K. Srivastava, R. Raghvir, C. M. Tripathi, (2013) Synthesis, characterization and biological activity of new cyclization products of 3-(4-substituted benzylidene)-2*H*-pyrido[1,2-*a*]pyrimidine

- 2,4-(3*H*)-diones, *Journal of Chemical Sciences*, **125**: 305-312.
23. R. K. Howe, B. R. Shelton, (1990) Spiroheterocycles from the reaction of nitrile oxides with 3-methylenephthalimides, *The Journal of Organic Chemistry*, **55**: 4603-4607.
 24. I. Batool, A. Saeed, I. Z. Qureshi, S. A. Razzaq, (2015) Synthesis, molecular docking and biological evaluation of new thiazolopyrimidine carboxylates as potential antidiabetic and antibacterial agents, *Research on Chemical Intermediates*, **42**: 1139-1163.
 25. G. Valarmathy, R. Subbalakshmi, (2013) Synthesis, spectral characterization and biological studies of novel schiff base complexes derived from 4,6-dimethyl-2-sulfanilamidopyrimidine and 2-hydroxy-3-methoxybenzaldehyde, *International Journal of Pharma and Bio Sciences*, **4(3)**: 287-295.
 26. R. R. Patel, V. G. Patel, (2010) Synthesis, characterization, chelating properties and antimicrobial activity of pyrimidine-phthalic anhydride combined molecule, *Rasayan Journal of Chemistry*, **3**: 188-193.
 27. N. P. Singh, A. N. Srivastava, (2013) Synthesis, characterization and antimicrobial studies of novel binuclear transition metal complexes of Schiff base derived from 1-amino-5-methyl-2, 6-pyrimidine-dione and 2, 3-butanedione, *Asian Journal of Chemistry*, **25**: 533-537.
 28. C. M. Sharaby, G. C. Mohamed, M. M. Omar, (2007) Preparation and spectroscopic characterization of novel cyclodiphosph (V) azane of N^1 -2-pyrimidinylsulfanilamide complexes: Magnetic, thermal and biological activity studie, *Spectrochimica Acta A*, **66**: 935-948.
 29. K. Singh, Y. Kumar, P. Puri, M. Kumar, C. Sharma, (2012) Cobalt, nickel, copper and zinc complexes with 1,3-diphenyl-1*H*-pyrazole-4-carboxaldehyde Schiff bases: Antimicrobial, spectroscopic, thermal and fluorescence studies, *European Journal of Medicinal Chemistry*, **52**: 313-321.
 30. R. Pradhan, M. Banik, D. B. Cordes, M. Z. Alexandra, S. N. C. Saha, (2015) Synthesis, characterization, X-ray crystallography and DNA binding activities of Co(III) and Cu(II) complexes with a pyrimidine-based Schiff base ligand, *Inorganica Chimica Acta*, **442**: 70-80.
 31. N. Revathi, M. Sankarganesh, J. P. Rajesh, J. D. Raja, (2017) Biologically active Cu(II), Co(II), Ni(II) and Zn(II) complexes of pyrimidine derivative Schiff base: DNA binding, antioxidant, antibacterial and *in vitro* anticancer studies, *Journal of Fluorescence*, 1-14. DOI: 10.1007/s10895-017-2118-y.
 32. J. G. Małecki, (2010) Synthesis, molecular and electronic structures of half-sandwich ruthenium(II) complexes with pyrimidine-based ligands, *Transition Metal Chemistry*, **35**: 801-808.
 33. B. Moreno-Lara, S. A. Carabineiro, P. Krishnamoorthy, A. M. Rodríguez, J. F. Mano, B. R. Manzano, F. A. Jálón, P. T. Gomes, (2015) Nickel(II) complexes of bidentate N-N' ligands containing mixed pyrazole, pyrimidine and pyridine aromatic rings as catalysts for ethylene polymerisation, *Journal of Organometallic Chemistry*, **799**: 90-98.
 34. R. A. A. Cassaro, M. Baskett, P. M. Lahti, (2013) Synthesis and characterization of new complexes derived from 4-thienylsubstituted pyrimidines, *Polyhedron*, **64**: 231-237.
 35. A. Ayadi, A. Jaafar, A. Fix-Tailler, G. Ibrahim, G. Larcher, A. El-Ghayoury, (2017) Tetrathiafulvalene based electroactive ligands and complexes: Synthesis, crystal structures and antifungal activity, *Tetrahedron*, **73**: 3554-3563.
 36. H. Dong, X. Liu, B. Zheng, Y. Wang, B. Ling, Z. Pin, J. Bi, S. Gou, (2015) Metallosupramolecular silver and zinc complexes with flexible or semirigid tripodal pyridyl pyrimidine ligands, *Journal of Inorganic and Organometallic Polymers and Materials*, **25**: 318-326.
 37. A. Leprêtre, A. Turck, N. Ple, G. Queguiner, (2000) Synthesis in the nitrogenp-De@cient heterocycles series using a barbier type reaction under sonication. Diazines, *Tetrahedron*, **56**: 3709-3715.
 38. H. Gajanan, H. P. Shivarudrappa, S. Yallappa, T. Venkatesh, S. Y. Nagendra, B. B. Raj, R. M. Shafeeulla, B. L. Dhananjaya, (2016) Synthesis and characterization of novel pyridinimine-based Schiff Base ligands and their Cu(II) complexes for biomedical application, *World Journal of Pharmaceutical Research*, **5(9)**: 715-729.
 39. R. M. Shafeeulla, G. Krishnamurthy, H. S. Bhojyanaik, H. P. Shivarudrappa, Y. Shiralgi, (2017) Spectral thermal cytotoxic and molecular docking studies of N^1 -2-hydroxybenzoyl; pyridine-4-carbohydrazide its complexes, *Beni-Suef University Journal of Basic and Applied Sciences*. DOI: ORG/10.1016/J.BJBAS.2017.06.001
 40. R. M. Shafeeulla, G. Krishnamurthy, H. S. Bhojyanaik, T. Manjuraj, (2016) Synthesis, cytotoxicity, and molecular docking study of complexes containing thiazole moiety, *Journal of the Turkish Chemical Society*, **4(3)**: 787-810.
 41. M. Bhat, G. K. Nagaraja, R. Kayarmar, S. K. Peethamber, R. M. Shafeeulla, (2016) Design, synthesis and characterization of new 1,2,3-triazolyl pyrazole derivatives as potential antimicrobial agents via a vilsmeier-haack reaction approach, *RSC Advances*, **6**: 59375-59388.

42. S. B. Patil, G. Krishnamurthy, H. S. B. Naik, R. L. Prashant, M. Ghate, (2010) Synthesis, characterization and antimicrobial studies of 2-(4-methoxy-phenyl)-5-methyl-4-(2-arylsulfanyl-ethyl)-2,4-dihydro-[1,2,4] triazolo-3-ones and their corresponding sulfones, *European Journal of Medicinal Chemistry*, **45**: 3329-3334.
43. N. D. Shashikumar, G. Krishnamurthy, H. S. B. Naik, M. R. Lokesh, K. S. J. Kumara, (2014) Synthesis of new biphenyl-substituted quinoline derivatives, preliminary screening and docking studies, *Journal of Chemical Sciences*, **126**: 205-212.
44. T. Manjuraj, G. Krishnamurthy, Y. D. Bodke, H. S. B. Naik, (2017) Metal complexes of quinolin-8-yl [(5-methoxy-1H-benzimidazol-2-yl) sulfanyl]acetate: Spectral, XRD, thermal, cytotoxic, molecular docking and biological evaluation, *Journal of Molecular Structure*, **1148**: 231-237.
45. D. H. William, I. Fleming, (1973) *Spectroscopic Methods in Organic Chemistry*, London, New York: McGraw-Hill.
46. R. Venkatraman, M. A. Hossain, F. R. Fronczek, (2010) {4-Phenyl-1-[1-(1,3-thiazol-2-yl) ethylidene] thiosemicarbazidato} {4-phenyl-1-[1-(1,3-thiazol-2-yl) ethylidene] thiosemicarbazide} nickel(II) chloride monohydrate, *Acta Crystallographica*, **66(5)**: 541-542.
47. K. Nakamoto, (1970) *Infrared Spectra of Inorganic and Coordination Compounds*, New York: John Wiley.
48. A. Kriza, L. V. Ababei, N. Cioatera, I. Rau, N. Stanica, (2010) Synthesis and characterization of some 1,2,4-triazole-3-thiones obtained from intramolecular cyclization of new 1-(4-(4-X-phenylsulfonyl)benzoyl)-4-(4-iodophenyl)-3-thiosemicarbazides, *Journal of the Serbian Chemical Society*, **75**: 229.
49. R. C. Maurya, P. Patel, (1996) Synthesis, magnetic and special studies of some novel metal complexes of Cu(II), Ni(II), Co(II), Zn(II), Nd(III) and U(VI) O₂ with Schiff base derived from sulfa drugs, *Spectroscopy Letters*, **32(2)**: 213-236.
50. S. M. El-Shiekh, M. M. Abd-Elzaher, M. Eweis, (2006) Synthesis, characterization and biocidal studies of new ferrocenylthiadiazolo-triazinone complexes, *Applied Organometallic Chemistry*, **20(8)**: 505-511.
51. B. D. Cullity, (1978) *Elements of X-ray Diffraction*, Reading, MA: Addison-Wesley.
52. R. M. Shafeeulla, G. Krishnamurthy, H. S. Bhojyanaik, T. C. M. Yuvaraj Manjunath Bhat (2017), Synthesis of 3-methyl-1-phenyl-4-(thiazol-2-yl)-1H-pyrazol-5(4H)-one via Sandmeyer Reaction and their Transition Metal Complexes; Spectral, XRD, Cytotoxicity, Molecular Docking and Biological Evaluation, *Der Pharma Chemica*, **9(15)**:19-26.
53. E. E. Erdem, Y. Sari, R. K. Arslan, N. Kabay, (2009) Synthesis and characterization of azo-linked Schiff bases and their nickel(II), copper(II), and zinc(II) complexes, *Transition Metal Chemistry*, **34**: 167-174.
54. T. A. Yousef, G. M. Abu El-Reash, O. A. El-Gammal, R. A. Bedier, (2013) Spectral studies of copper(II) complexes of 6-(3-thienyl) pyridine-2-thiosemicarbazone, *Journal of Molecular Structure*, **1035**: 307.